Biodegradation (2006) 17: 357–367
DOI 10.1007/s10532-005-9006-x
© Springer 2006

Bio-deposition of a calcium carbonate layer on degraded limestone by *Bacillus* species

Jan Dick[1], Wim De Windt[1], Bernard De Graef[2], Hans Saveyn[3], Paul Van der Meeren[3], Nele De Belie[2] & Willy Verstraete[1]*
[1]*Laboratory of Microbial Ecology and Technology (LabMET), Ghent University, Coupure Links 653, B-9000 Ghent, Belgium;* [2]*Magnel Laboratory for Concrete Research, Dept. of Structural Engineering, Ghent University, Technologiepark Zwijnaarde 904, B-9052 Ghent, Belgium;* [3]*Laboratory of Applied Physical Chemistry, Particle and Interfacal Technology Group, Ghent University, Coupure links 653, B-9000 Ghent, Belgium (*author for correspondence: e-mail: Willy.Verstraete@UGent.be)*

Accepted 18 July 2005

Key words: biofilm, biomineralisation, $CaCO_3$, urea degrading activity, ζ-potential

Abstract

To obtain a restoring and protective calcite layer on degraded limestone, five different strains of the *Bacillus sphaericus* group and one strain of *Bacillus lentus* were tested for their ureolytic driven calcium carbonate precipitation. Although all the *Bacillus* strains were capable of depositing calcium carbonate, differences occurred in the amount of precipitated calcium carbonate on agar plate colonies. Seven parameters involved in the process were examined: calcite deposition on limestone cubes, pH increase, urea degrading capacity, extracellular polymeric substances (EPS)-production, biofilm formation, ζ-potential and deposition of dense crystal layers. The strain selection for optimal deposition of a dense $CaCO_3$ layer on limestone, was based on decrease in water absorption rate by treated limestone. Not all of the bacterial strains were effective in the restoration of deteriorated Euville limestone. The best calcite precipitating strains were characterised by high ureolytic efficiency, homogeneous calcite deposition on limestone cubes and a very negative ζ-potential.

Introduction

The natural and anthropogenic erosive impact on limestone is high, due to the high receptivity of the fragile calcium carbonate matrix. Since the Industrial Revolution, NO_x and SO_x pollution causes an acidification of the rain, dissolving the calcite. Wind and dust cause an eroding effect on limestone due to the continuous physical erosion of the surface (Warscheid & Braams 2000).

A novel strategy to restore corroded limestone is biomineralisation of calcium carbonate. Biomineralisation is defined as a biologically induced precipitation in which an organism creates a local micro-environment, with conditions that allow optimal extracellular chemical precipitation of mineral phases (Hamilton 2003). Species of the *Bacillus* group are able to precipitate calcite on their cell constituents and in their micro-environment by conversion of urea into ammonia and carbon dioxide (Castanier et al. 1999; Hammes et al. 2003). The bacterial degradation of urea locally increases the pH and promotes the microbial deposition of carbon dioxide as calcium carbonate in a calcium rich environment (Warren et al. 2001).

The basic reaction of the calcocarbonic system is:

$$CO_3^{2-} + Ca^{2+} \longleftrightarrow CaCO_3 \ (K_{so} = 3.8 * 10^9) \quad (1)$$

with K_{so} the solubility product.

The driving force for precipitation of $CaCO_3$ is the supersaturation level S, defined by the ratio of the ionic product:

$$S = (Ca^{2+})x(CO_3^{2-})/K_{so} \quad (2)$$

During microbial urease activity, 1 mole of urea is hydrolysed intracellularly to 1 mole of ammonia and 1 mole of carbamate (Eq. 3), which spontaneously hydrolyses to form an additional 1 mole of ammonia and carbonic acid (Eq. 4) (Burne & Chen 2000).

$$CO(NH_2)_2 + H_2O \longrightarrow NH_2COOH + NH_3 \quad (3)$$

$$NH_2COOH + H_2O \longrightarrow NH_3 + H_2CO_3 \quad (4)$$

These products subsequently equilibrate in water to form bicarbonate and 2 moles of ammonium and hydroxide ions (Eqs. 5 and 6).

$$H_2CO_3 \longleftrightarrow HCO_3^- + H^+ (pK_{a2} = 6.37) \quad (5)$$

$$2NH_3 + 2H_2O \longleftrightarrow 2NH_4^+ + 2OH^- \quad (6)$$

The latter 2 reactions give rise to a pH increase, which in turn shifts the bicarbonate equilibrium, resulting in the formation of carbonate ions (Eq. 7). This pH increase takes place initially in the local micro-environment around the bacterial cell, and propagates in the bulk solution of the bacterial cell suspension.

$$HCO_3^- + H^+ + 2NH_4^+ + 2OH^- \longleftrightarrow CO_3^{2-} + 2NH_4^+ + 2H_2O \quad (7)$$

Thus, the carbonate concentration will increase, inducing an increase in S (according to Eq. 2) and resulting in $CaCO_3$ precipitation around the cell, in the presence of soluble calcium ions. The purpose of this study was to identify the key factors in the optimal biological calcium carbonate precipitation on limestone. The latter can subsequently be used as criteria for the selection of *B. sphaericus* strains in future research efforts to optimise bio-deposition of calcium carbonate ($CaCO_3$). The biological key factors had to be easy in use, and applicable for quick screening, contrary to the slow chemico-physical structural analyses.

Materials and methods

Selection of the limestone

Euville limestone is often used for building and sculpturing. Euville is excavated in the 'Département de la Meuse' in France. The stone has a rough granulated structure and was created by a mixture of fossilised crinoids and echinoids, cemented together by crystalline calcium carbonate. A characteristic feature of Euville stone is its high water absorption.

Bacterial strains and culture conditions

Five different isolates of the *Bacillus sphaericus* group and one *Bacillus lentus* isolate were examined for their capacity to deposit a calcium carbonate layer on limestone. Those strains were isolated from a calcareous sludge from a biocatalytic ureolytic calcification reactor, according to the protocol described by Hammes et al. (2003). In brief, samples were suspended in a sterile physiological solution (8.5 g l^{-1} NaCl (VWR International, Leuven, Belgium)), diluted appropriately and plated on precipitation agar. Colonies were assessed every 5 days with a stereomicroscope (WILD, Heerbrugge, Switzerland) and positive colonies were selected based on visual crystal formation within 10 days. Positive isolates were purified by repetitive dilution and plating. Based on their morphology, 6 unique strains were obtained. Rowan et al. (2003) suggested that these strains could be identified by using an API CHB test kit (BioMérieux, Marcy-l'Etoile, France). According to their biochemical properties, these tests identified the isolates as species of the *Bacillus sphaericus* group. The purified isolates were additionally identified by DNA sequencing according to the RNA extraction from soil with mini-beadbeater protocol (Griffiths et al. 2000; Kowalchuk et al. 1998) and the DNA sequences were deposited to the National Center for Biotechnology Information (NCBI). The isolates were deposited in the Belgian Co-ordinated Collections of Micro-organisms culture collection (BCCM Ghent, Belgium). The corresponding numbers are listed in Table 1. For ease of reading, strains were designated common names by means of their abbreviated BCCM numbers: strain 55, 56, 57, 58, 59 and 60.

Table 1. Identification of the six strains used in this study and the respective catalogue numbers in the deposited collections

Species	Common number	BCCM number	Accession number
Bacillus sphaericus	55	LMG 222 55	Not available
Bacillus sphaericus	56	LMG 222 56	AY 766328
Bacillus sphaericus	57	LMG 222 57	AY 766327
Bacillus sphaericus	58	LMG 222 58	AY 766325
Bacillus sphaericus	59	LMG 222 59	AT 766324
Bacillus lentus	60	LMG 222 60	AY 766326

Liquid culture media consisted of 3 g l^{-1} Nutrient Broth (Oxoid N.V., Drongen, Belgium), 2.12 g l^{-1} $NaHCO_3$ (VWR International, Leuven, Belgium) and 10 g l^{-1} urea (VWR International, Leuven, Belgium). To solidify media, 20 g l^{-1} agar (Oxoid N.V., Drongen, Belgium) was added (Stocks-Fischer et al. 1999). To avoid the possible ammonia toxicity towards *B. lentus*, the ammonia was captured out of the reactors with growth medium by means of tubes, open at the top and filled with 12 N H_2SO_4 (VWR International, Leuven, Belgium), that did not come in contact at any time with the growth medium. The evaporated ammonia was captured by the sulphuric acid as ammonium (Eqs. 8–9).

$$CO(NH_2)_2 \longrightarrow NH_3 + CO_2 \qquad (8)$$

$$NH_3 + H_2SO_4 \longrightarrow NH_4^+ + HSO_4^- \qquad (9)$$

All incubations were done at 28 ± 2 °C on a shaker at 100 rpm.

Microscopic inspection of calcium carbonate produced on agar plates

Different isolates were plated from a liquid culture on agar plates with 7.5 g l^{-1} $CaCl_2 \cdot 2H_2O$ (VWR International, Leuven, Belgium) (Stocks-Fischer et al. 1999). The calcium carbonate encrustations were observed with a stereomicroscope (WILD, Heerbrugge, Switzerland).

Total ammonium nitrogen and optical density measurement

The production of ammonia by different *Bacillus* isolates was measured as a function of growth in liquid culture medium. After a 10% (v/v) inoculation with an overnight culture, samples were taken from 3 biological replicates every 3 h for optical density (OD) and total ammonium nitrogen (TAN) measurements. To obtain the chemical degradation of urea as control, non-inoculated aliquots were set up ($n = 3$) and analysed by the same procedures. In order to assess the growth, the optical density was measured with a spectrophotometer (Dr. Lange ISiS9000, Hegnau, Switzerland) at 588 nm. TAN concentrations were measured colorimetrically by the method of Nessler (Greenberg et al. 1992). The specific urea degradation rate (SUD) was defined as the ratio of ammonium production (AP) per unit of bacterial growth in a given time (t) and is given by the following formula:

$$SUD = \frac{AP(\text{g ammonium} \times l^{-1})}{[OD_{cells}] \times t(h)} \qquad (10)$$

Extracellular polymeric substances-production

Extracellular polymeric substances (EPS) production was tested according to the procedure described by Friedman et al (2001). Briefly, the dye Congo red was mixed in a 48 h *Bacillus* culture at a concentration of 3.5 mg l^{-1} in order to stain EPS-producing *Bacillus* strains and the aliquots were incubated for 30 min ($n = 3$). The coloured culture was centrifuged for 2 min at 12,110 × *g* (Eppendorf Mini-Spin, Hamburg, Germany) to harvest the dyed cells. The cells were washed with 1 ml of deionised water to release adsorbed Congo Red into the water. To remove the cells, the dyed culture was centrifuged for 2 min at 12,110 × *g* (Eppendorf MiniSpin, Hamburg, Germany). The supernatant was measured at 430 nm with a spectrophotometer (Dr. Lange ISiS9000, Hegnau, Switzerland). Destilled water was used as negative control. The increase in absorbance is due to the uptake of Congo red by the EPS producing bacteria.

Biofilm production

Bacillus biofilms were established aseptically in 1/10 Nutrient Broth, supplemented with 2.12 g l^{-1}

$NaHCO_3$ and 10 g l^{-1} urea (Molin & Molin 1997) on glass plates (7×25 mm) in a flow system (n = 3). The flow cell was initially sterilised by rinsing whith NaOCl, 70% ethanol and sterilised deionised water. The growth chamber was inoculated with 10 % (v/v) of an overnight culture at OD_{588} 0.5 and 1 h of stagnation was applied to allow initial adhesion of the bacterial cells to the glass. After initial attachment of cells, the medium was pumped through the flow channels at a rate of 0.5 ml min^{-1} using a peristaltic pump (Watson Marlow type 505S, Cornwall, England). When a mature biofilm was obtained (120 h), the glass plates were collected. Media and loosely bound cells were removed from the glass plate by gently rinsing with sterile distilled water.

The adherent bacterial cells were stained with a 0.1% crystal violet solution for 1 min at room temperature. The superfluous dye was removed by two rinses with distilled water. The bound crystal violet was extracted from the stained cells with 3 ml 99% ethanol. The biofilm was quantified by measuring the absorbance of the solution at 430 nm (Wen & Burne 2002).

ζ-potential evolution

The ζ-potential of bacteria is a measure for their surface potential originating from (de)protonation or (de)complexation of surface molecules such as polysaccharides or proteins. It can be calculated from the measured electrophoretic mobility under a known electric field. Cultures were grown in liquid defined medium, containing 2 g l^{-1} NH_4Cl for 24 h for optimal growth conditions (Hammes et al. 2003). The pH of 50 ml aliquots of overnight *Bacillus* sp. cultures was adjusted with 12 N HCl (VWR International, Leuven, Belgium) and electrophoretic mobility (μ) was measured at pH 6, 7, 8 and 9, respectively with a Malvern Zetasizer IIc (Malvern, Worcestershire, United Kingdom) device at 25 °C and an applied electric field strength of 2000 V m^{-1} using the Helmholtz-Smoluchouski equation (Tsuneda et al. 2003):

$$\zeta = \frac{\mu \times \eta}{\varepsilon_0 \times \varepsilon_r} \qquad (11)$$

with: μ being the electrophoretic mobility (m^2 s^{-1} V^{-1}); ε_0 being the permittivity of vacuum (C^2 J^{-1} m^{-1}); ε_r being the dielectric constant; ζ being the ζ-potential (V); η being the viscosity (kg m^{-1} s^{-1}).

Adhesion of the newly formed layer to the surface

On Euville limestone, a calcium carbonate layer was biologically deposited on the corroded surface, in order to test the remediation potential of the different *Bacillus* strains. Limestone cubes (70×30×30 mm) were incubated in airtight sterilised jars with liquid medium, inoculated with 1% of the different *Bacillus* strains (n = 3). No carbonate was initially present in the system, since double-deionized (milliQ) water was used for culture broth preparation. The surface was rewetted by shaking 5 min with an interval of 2 h at 100 rpm to create optimal conditions to grow a biofilm. After two weeks $CaCl_2$ was added to the medium, in a final concentration of 7.5 g l^{-1}, in order to precipitate calcium carbonate onto the biofilm. The third week, the limestone cubes were suspended in fresh medium in order to have a second phase of biofilm growth. As before, the medium was inoculated with the respective strains. In the fourth week, by adding 7.5 g l^{-1} $CaCl_2$, a new calcite layer was deposited onto the primary precipitated calcite layer to smoothen the surface. Finally, the cubes were dried at 200 °C to obtain a dry calcium carbonate crystal structure. The sterile control consisted of limestone cubes exposed to the same treatment as described above in a sterile environment, with only chemical precipitation of $CaCO_3$.

Scanning electron microscopy (SEM)

SEM of limestone cubes, to visualise the deposited calcite crystals after treatment, was done with a JEOL JSM5600LV scanning electron microscope (Massachusetts, USA).

Ca-removal in ureolytic cultures

Limestone cubes (10×30×30 mm) were attached to sterile jars, filled with the *Bacillus* medium and airtight incubated after inoculation with a 10% (v/v) *Bacillus* strain (n = 3). After 24 h of growth, the liquid was removed and fresh *Bacillus* medium was added, including 7.5 g l^{-1} $CaCl_2$ at pH 5. No $NaHCO_3$ was used to suppress the chemical $CaCO_3$ precipitation. Every 2 h, samples

were taken from the bulk for calcium analysis and pH, up to 22 h after the start-up. Samples from the bulk solution were diluted to the appropriate concentration in 50 ml flasks and analysed with a Perkin Elmer AAS 3110 apparatus (Norwalk, USA).

Water absorption of the treated limestone surface

The limestone specimens were coated at the four edges adjacent to the treated side, to ensure unidirectional absorption through the treated side. The coating (Dekguard, Tamworth, UK) consisted of two layers of polysiloxane and one layer of siliconpaint. After coating, the test cubes were dried at 70 °C in a ventilated kiln, establishing a mass change of less than 0.1% between two measurements at 24 h intervals, to ensure low uniform moisture content in the limestone matrix. The specimens were submerged, to 10 ± 1 mm of water, with the treated side facing downwards, in an atmosphere of 20 °C and relative humidity of 60%. At regular time intervals, the specimens were removed from the water and the mass of water absorbed was determined using an electronic balance. The test cubes were weighed every half hour for the first 4 h of the test, then every hour until 8 h after the beginning of the test and after 24, 32, 48, 56, 72, 80, 96, 108, 168 and 216 h of the test. The measurements were performed after removing excessive water from the surface with a moist towel. In order to determine the maximum absorption level, a vacuum saturation was applied on the specimens during 2.5 h. Afterwards, water was injected so that the samples were completely submerged within 1 h. This submerged state remained for another 24 h. This vacuum absorption test was concluded with measuring the surface-dry weight of the samples.

The capillary water absorption $E_{c,t}$ during the first part of the experiment is expressed as:

$$E_{c,t} = \frac{m_t - m_1}{m_1} \times 100 \quad (\%) \tag{12}$$

while the water absorption under vacuum E_v is expressed as:

$$E_v = \frac{m_v - m_1}{m_1} \times 100 \quad (\%) \tag{13}$$

with m_1 the initial mass of the test cube after drying in the oven at 70 °C; m_t the mass at time t and m_v the mass after water absorption under vacuum.

The results of the capillary absorption measurement can then be expressed as the relative impregnation rate (S_t) on a certain moment t:

$$S_t = \frac{E_{c,t}}{E_v} \times 100 \quad (\%) \tag{14}$$

Statistical analysis

To perform different statistical analysis the programmes SPSS6 and Microsoft Excel were used.

Results

Visualisation of specific calcite production

To determine the efficiency of calcium carbonate precipitation by the six isolates, a dilution series of each was plated on solid media containing $CaCl_2$. The calcium carbonate precipitation was visualised as a mineral crust on the colonies. The mineral precipitation of the different colonies after 3 days is visualised in Figure 1. Based on microscopic inspection, strains 57 and 59 produced large crystal aggregates at about 95% of the surface. Strain 56 produced large crystals at about 75% of the colony surface. Strains 55, 58 and 60 have the lowest calcite deposition onto plate colonies, only at the centre calcium carbonate was precipitated.

Ca-removal in ureolytic cultures

During the urea degradation the pH started to rise within the first 4 h to a pH of 8.4 ± 0.1 and gradually to pH 9.0 ± 0.2 after 16 h for all the strains of the *Bacillus sphaericus* group. The outgroup, *Bacillus lentus*, produced a slow increase to a final pH of 8.0 ± 0.6. The pH in the negative control rose in an initial phase to 6.3 ± 0.4, but after 18 h the pH started to rise towards a final pH of 7.3 ± 0.1 (Figure 2). The augmented carbonate concentration and the rise in pH caused a precipitation of calcium carbonate. The decline of the initial calcium concentration of 7.5 ± 0.5 g l^{-1} in the bulk fluid over 22 h is shown in Figure 3. After 10 h of incubation, 3 significant groups could be distinguished. Strains

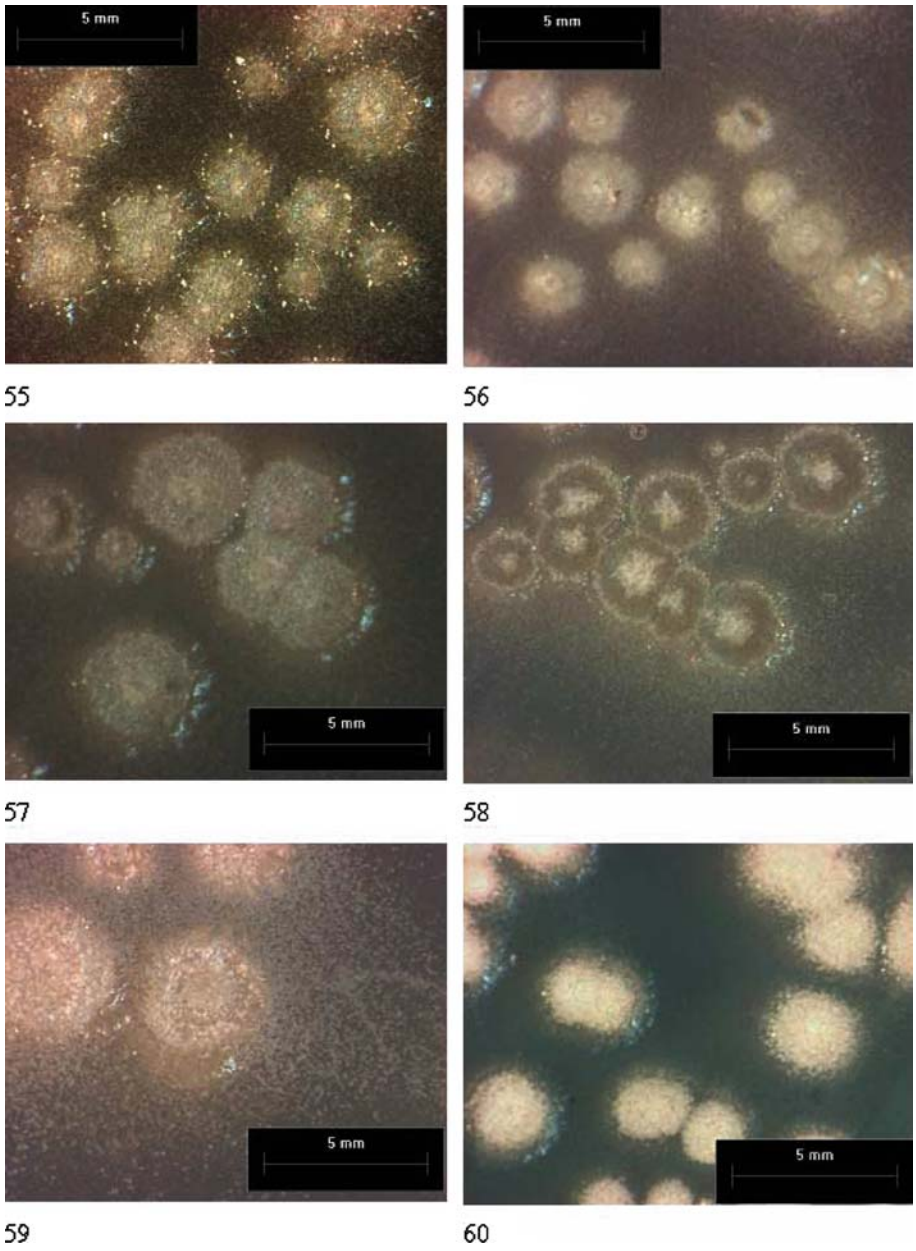

Figure 1. These illustrations show colonies of 6 different strains of *B. sphaericus* and *B. lentus* on agar plates and their ability to encrust themselves in a calcium carbonate.

55, 56 and 58 induced a quick calcium precipitation after 4 h. The strains 57 and 59 had a slower calcium removal rate and started to remove the calcium after 10 h. While 60 showed a very slow calcium carbonate precipitation, it started after only 12 h to precipitate calcium and only a final calcium concentration in the liquid of 3.35 ± 0.48 g l^{-1} was reached.

Urea degrading capacity

All the different isolates of the *Bacillus* group were tested for their growth on a urea containing medium. Only strain 60 exhibited slow growth. When the ammonia was stripped out of the medium and captured into sulphuric acid, 60 was growing to a dense culture (data not shown). The

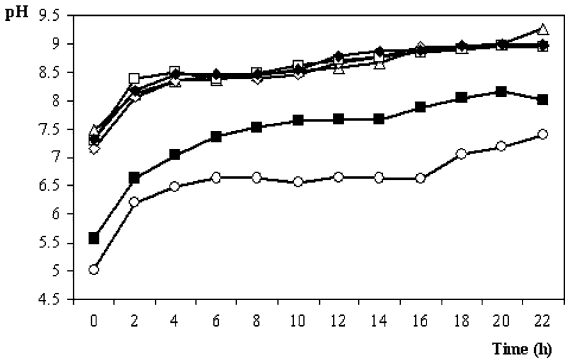

Figure 2. Increase of pH due to urea degradation by the different *Bacillus* strains. Each value represents the mean value of 3 independent replicates for treatment with: (Δ) 55; (▲) 56; (◇) 57; (□) 58; (♦) 59; (■) 60 and (○) sterile control.

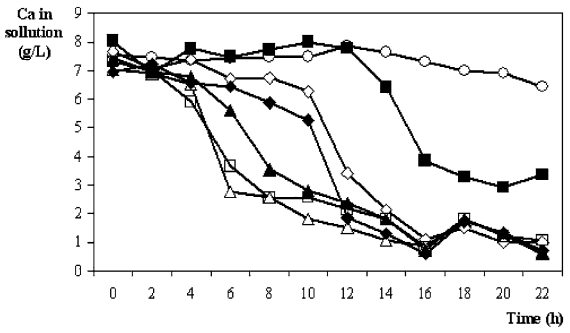

Figure 3. Calcium removal by formation of calcium carbonate after urea degradation. Each value represents the mean value of 3 independent replicates for treatment with: (Δ) 55; (▲) 56; (◇) 57; (□) 58; (♦) 59; (■) 60 and (○) sterile control.

urea degrading activity of the different bacteria after 49 h is listed in Table 2. Three significant groups could be distinguished ($p < 0.05$). Group 1, consisting of 55, 56 and 57, produced TAN levels up to 4.77 ± 0.13 g l^{-1}. Group 2, strains 58 and 59, produced TAN levels up to 4.02 ± 0.05 g l^{-1}. Group 3, represented by 60, showed almost no urease activity. The chemical decomposition of urea under the conditions of the test remained at 0.76 ± 0.12 g l^{-1}. The specific urea degradation of the different strains is illustrated in Figure 4a and b and significant differences between the 6 strains

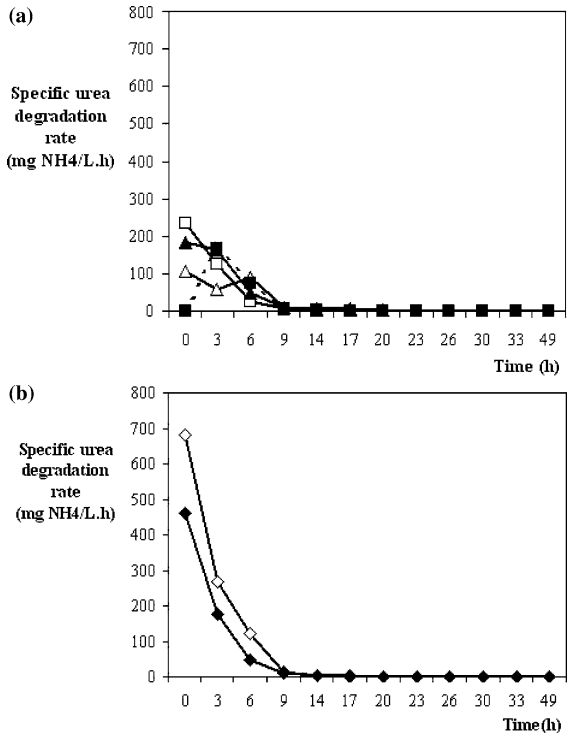

Figure 4. (a) The specific urea degradation rate for strains with a high initial value. (b) The specific urea degradation rate for strains with al low initial value. (Δ) LMG 222 55; (▲) LMG 222 56; (◇) LMG 222 57; (□) LMG 222 58; (♦) LMG 222 59; (■) LMG 222 60; no error bars were added to keep the figure simple, values represent the mean of 3 biological replicates.

Table 2. Overview of the different key-factors and their mean value ± standard deviation for six isolates of the *Bacillus* species.

Strain number	ζ-potential (mV) at pH 9	Urea degradation after 49 h (g NH_4–N l^{-1})	EPS- production[a]	Biofilm production (CFU mm^{-2})
55	−8.78 ± 0.29	4.76 ± 0.06	0.09 ± 0.01	$(1.4 \pm 1.0)\cdot10^2$
56	−24.90 ± 4.17	4.65 ± 0.02	0.12 ± 0.02	$(1.4 \pm 1.1)\cdot10^2$
57	−27.78 ± 1.73	4.90 ± 0.12	0.09 ± 0.01	$(1.6 \pm 0.5)\cdot10^2$
58	−13.96 ± 0.58	3.98 ± 0.41	0.12 ± 0.01	$(2.7 \pm 0.5)\cdot10^2$
59	−23.03 ± 1.01	4.07 ± 0.15	0.12 ± 0.01	$(3.2 \pm 0.6)\cdot10^2$
60	−13.53 ± 0.72	0.82 ± 0.0.04	0.08 ± 0.01	$(1.4 \pm 1.0)\cdot10^2$

[a]EPS = Extracellular Polymeric Substances.

were observed during the first 6 h of growth and urea degradation. Strains 55, 56, 58 and 60 exhibited a low specific urea degrading activity. The initial specific activity started at 105 ± 28 g NH_4^+ l^{-1} h^{-1} for strain 55, 184 ± 6 g NH_4^+ l^{-1} h^{-1} for strain 56 and 236 ± 30 g NH_4^+ l^{-1} h^{-1} for strain 58. Strain 57 had a specific urea degradation capacity of 459 ± 13 g NH_4^+ l^{-1} h^{-1} and strain 59 reached 807 ± 3 g NH_4^+ l^{-1} h^{-1}. After 3 h the specific ureolytic degradation rate decreased to 59 ± 12 g NH_4^+ l^{-1} h^{-1} for strain 55, to 165 ± 3 g NH_4^+ l^{-1} h^{-1} for strain 56, to 269 ± 2 g NH_4^+ l^{-1} h^{-1} for strain 57 and to 125 ± 12 g NH_4^+ l^{-1} h^{-1} for strain 58. Strain 59 had a specific urea degradation rate of 176 ± 7 g NH_4^+ l^{-1} h^{-1}.

EPS-production

Based on absorbance (430 nm) of the supernatant with extracted Congo red (Table 2), no biologically significant influences were observed between all different strains.

Biofilm production

In Table 2, the results of a 5 day biofilm density study are shown, after which a mature sessile community was obtained. Monoxenic biofilms of 58 and 59 contained 270 and 320 CFU mm^{-2} respectively. Strains 55, 56, 57 and 60 were less effective in covering the surface, with 140–160 CFU mm^{-2}, but these results were not biologically significant.

ζ-potential

The cell surface electric properties are listed in Table 2. At pH 6 and 7, the negative ζ-potential is similar for all the strains, although 56 and 57 were more negatively charged (data not shown). Also at pH 8, strain 57 had the most negative ζ-potential (data not shown). Since pH rises due to the ureolytic activity, the ζ-potential is relevant for this study only at pH 9. At this pH, a significant difference ($p > 0.05$, Student T-test) was found between 3 groups. Strains 56, 57 and 59 had the most negative ζ-potential, 55 had the least negative ζ-potential and 58 and 60 had an average ζ-potential.

Water absorption of the treated limestone surface

The capillary water absorption of the limestone cubes, treated with the different strains, was tested over a period of 5 days. The saturation curves of the initial phase, over 8 h, are indicated in Figure 5. After 2 days, the water capillarity of the cubes started to approach a constant value of 64 ± 4% (data not shown). Three groups could be distinguished, based on the first 8 h. One group consisted of the sterile control and samples treated with 55 and 56, exhibiting the highest initial capillary absorption. A second cluster represented 58 and 60 with a moderate absorption level. A third group included 57 and 59, with the lowest initial capillary water absorption.

Scanning Electon Microscopy of the treated surface

Two strains with the most and least beneficial impact on capillary water absorption by limestone, strains 59 and 58, respectively, were selected for SEM evaluation of the treated surface. By means of SEM, the crystal shape and distribution could be evaluated. Strain 59 exhibited a homogeneous calcite deposition of rhombohedrical attached crystals, whereas the deposition by strain 58 was characterised by dense curtains of calcite crystals that were heterogeneously distributed over the limestone surface (Figure 6a–c).

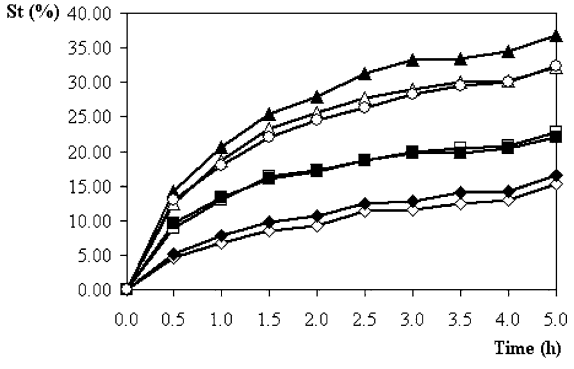

Figure 5. Initial water capillary absorption of untreated and treated limestone, correlated with the water repellent quality of the newly formed calcite layer. Each value represents the mean relative impregnation rate (S_t) of 3 independent replicates for treatment with: (Δ) 55; (▲) 56; (◇) 57; (□) 58; (♦) 59; (■) 60 and (○) sterile control.

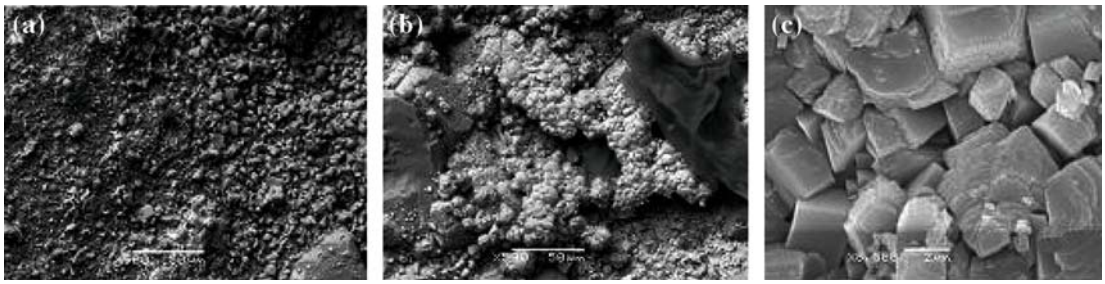

Figure 6. (a) Scanning Electron Microscopy (SEM) image of a dense and homogeneous layer of calcite crystals produced by *B. sphaericus* strain 59 on limestone; (b) SEM image of irregular calcite curtains produced by strain 58 on limestone; (c) Magnification of (a), in which the typical rhombohedrical shape of calcite was visualised.

Discussion

Limestone is an aggregation stone and consists of mineral material and pores. Pore volume and size determine the capacity for fluid storage and salt accumulation. Both factors are important for the further erosion and the durability of the stone. Frost weathering, by freeze and thaw action, and salt crystallisation are the main cause for the deterioration of stone (Caltrone et al. 2004; Prikryl et al. 2003). A decrease in the ability to absorb water will result in a deceleration of the weathering process. A thin restoring layer of calcite can act as an alternative for the natural calcite skin on the stone surface. Biologically produced by ureolytic activity, the calcite layer will clog the pores at the surface of the limestone to decrease the water absorption rate. The growth related microbiological urea degradation is the main source of inorganic carbon dioxide in calcium and carbonate oversaturated medium and the cause of calcium carbonate precipitation (Merz-Preiss & Riding 1999; Yates & Robbins 1999, Warren et al. 2001). Two of five isolated *Bacillus sphaericus* strains, 57 and 59, were effective in calcium carbonate precipitation to remediate Euville limestone. The purpose of this research was to identify the specific key-factors correlated with the decrease of water absorption capacity by the treated limestone, for fast screening of the strains. The studied key-factors were: calcite production on agar plates, urea degrading capacity, production of extra-polymer substances, biofilm production, production of dense crystals on limestone surfaces, increase in pH, calcium precipitation over 22 h and ζ-potential.

The homogeneity of the calcite layer precipitated on limestone was evaluated by SEM, and the pore-filling effect by capillary water absorption. Water absorption is the process whereby fluid is drawn into a porous unsaturated material under the action of capillary forces. The capillary suction depends on the pore volume and geometry, and the saturation level of the limestone. Actually such tests measure porosity which may be insensitive to the transport mechanisms influencing durability (Beushausen et al. 2003; Cultrone et al. 2004; Prikryl et al. 2003). A modified version of the sorptivity test is based on the Belgian norm NBN B 05-201, which is an indicator for frost resistance. In general, 57 and 59 were characterised by the best calcite deposition on agar plates, whereas on limestone these strains were very effective in precipitating a regular calcite layer to induce a decrease of capillary water uptake within 2 days. Strains 55 and 56 had a similar absorption level as the untreated stone. Strains 58 and 60 showed results in between those of the earlier mentioned groups. A small water uptake rate is of major importance for proof of limestone against short, intense water contact. After 2 days, all the tested cubes reached the same saturation level of $64 \pm 4\%$ (data not shown).

B. pasteurii, B. cereus and *B. sphaericus* can use urea as an energy source, resulting in the production of ammonia and carbonate (Mobley & Huasinger 1989). This increases the pH and the carbonate concentration near the cells, triggering Ca^{2+} and CO_3^{2-} to precipitate as $CaCO_3$ (Mobley & Huasinger 1989; Castanier et al. 1999; Hammes et al. 2003; Stocks-Fischer et al. 1999; Udert et al. 2003). *B. sphaericus* strains induced a fast pH increase and when limestone cubes, covered with active biofilm, were submerged in fresh liquid broth, there was an instantaneous pH increase due

to the release of ureolytic metabolites. The *B. lentus* strain exhibited a slower urease metabolism, coupled to a slow pH increase of the surrounding environment and thus poor $CaCO_3$ deposition on limestone cubes covered with a biofilm. Limestone in a sterile environment removed calcium from the surrounding bulk medium due to sorption or by leaching of H_2CO_3 from the limestone into the unbuffered bulk solution at pH 5. During concomitant pH increase, HCO_3^- reached the level at which supersaturation occurred and resulted in $CaCO_3$ precipitation into the sterile control reactors (Eq. 14):

$$Ca^{2+} + 2HCO_3^- \longleftrightarrow CaCO_3 + CO_2 + H_2O \quad (15)$$

The CO_2 produced in this process will escape to the headspace, until an equilibrium is reached.

The matrix of extracellular polymeric secretions (EPS) has been discribed to influence the calcium carbonate precipitation in a positive way (Kawaguchi & Decho 2002). EPS appears to play a role in the coverage of the surface by biofilms, cell adhesion (Tsuneda et al. 2003) and possibly the capturing of the produced calcium carbonate, which might result in a homogeneous layer of calcium carbonate. The importance of a biofilm is to colonize the surface of the stones and react as nucleation site for extracellular calcium carbonate precipitation (Merz-Preiss & Riding 1999). In our study, however, there were no significant differences in the ability of the six strains to form biofilms and to produce EPS, so the importance of these factors for the restoration of limestone could not be elucidated.

The factor with the greatest predictive power for screening *Bacillus* candidates for good limestone restoration, was the ζ-potential. The ζ-potential is a measure of the potential of the electric layer at the surface of the cells. The ζ-potential is an important factor in the adhesion and surface colonisation by bacteria. Due to the postive ζ-potential of the limestone, it will be an easier substratum for colonisation by bacteria with a highly negative ζ-potential (Amer et al. 1985). The ζ-potential of the limestone is similar for all the bacterial strains, but the colonisation capacity of the strain itself depends upon its negative ζ-potential. A more energetically favourable and thus easier approach of the substratum by the ureolytic bacteria will result in a denser layer of calcium carbonate (Stocks-Fischer et al. 1999). Although the ζ-potential was measured at pH 6, 7, 8 and 9, only pH 9 was of importance in this study, because pH 9 is the growth optimum for *B. sphaericus* and because the pH in the reactors increased to 9 very rapidly. At pH 9, strains 56, 57 and 59 had the most negative ζ-potential, which was almost three times the ζ-potential of strain 55. Interestingly, the ζ-potential values reflect the effect of the most strains on initial water capillary absorption. Strains 57 and 59, with the most negative ζ-potential, had the most pronounced effect on decrease in capillary absorption of limestone. Strains 58 and 60, with intermediary ζ-potential values, had an intermediary effect on initial water capillary absorption between the untreated controls and the effect of strains 57 and 59. And strains 55 and 56 had no significant impact on the limestone capillary absorption properties. Only for strain 56, there is no correlation between negative ζ-potential and the effect on the limestone absorption. This can probably be explained by the low initial urea degradation rate by strain 56. The specific urea degradation rate is the second important key factor investigated in this study. A high initial specific urea degradation rate is typical for bacteria with a high affinity for urea. This high affinity is typical for a high substrate turn-over at low biomass present.

It is the first time that ζ-potential and urea degradation rate of *Bacillus* strains have been linked to homogeneous surface colonization of limestone and fast precipitation of a $CaCO_3$ layer with a concomitantly decreased water absorption rate by the limestone. The combination of a very negative ζ-potential, a high initial urea degradation rate, high surface covering of colonies with $CaCO_3$ and a homogeneous precipitation of calcite on a limestone surface explains why strains 57 and 59 are most suited for limestone restoration and protection. These 4 parameters are easily determined and provide powerful microbiological selection criteria for the bio-restoration of limestone.

Conclusions

In this study, several key-factors involved in microbiological remediation and conservation of decayed limestone by the process of ureolytic

calcium precipitation were investigated. It was observed that *B. sphaericus* strains with a very negative ζ-potential, a high initial urea degradation and a continuous formation of dense calcium carbonate crystals are most suitable for coherent calcite production on degraded limestone. These strains also significantly decreased capillary water absorption of the treated limestone.

Acknowledgements

This work was supported by a grant from the Fund for Scientific Research – Flanders (project G.0054.02). The authors wish to thank Nico Boon, Sylvie Seurinck and Kim Windey for critically reading this manuscript.

References

Amer F, Mahoud AA & Sabet V (1985) Zeta-potential and surface-area of calcium carbonate as related to phosphate sorption. Soil Sci. Soc. Am. J. 49(5): 1137–1142

Beushausen HD, Alexander MG & Mackechnie J (2003) Aspekte der Dauerhaftigkeit des Betons in einem internationalen Vergleich. Concrete Precast Plant Technol. 7: 22–33

Burne RA & Chen YY (2000) Bacterial ureases in infectious diseases. Microbes Infect. 2: 533–542

Castanier S, Le Métayer-Levrel G & Perthuisot J (1999) Ca-carbonates precipitation and limestone genesis – the microbiogeologist point of view. Sediment. Geol. 126: 9–23

Cultrone G, Sebastian E, Elert K, de la Torre MJ, Cazalla O & Rodriguez-Navarro C (2004) Influence of mineralogy and firing temperature on the porosity of bricks. J. Eur. Cer. Soc. 24: 547–564

Friedman LE, de Passerini Rossi BN, Messina MT & Franco MA (2001) Phenotype evaluation of *Bordetella bronchiseptica* cultures by urease activity and congo red affinity. Lett. Appl. Microbiol. 33: 285–290

Greenberg AE, Clesceri LS & Eaton ED (1992) Standard methods for Examination of Water and Wastewater. 18American Public Health Association, Washington DC

Griffiths RI, Whitley AS, O'Donnell AG & Bailey MJ (2000) Rapid method for coextraction of DNA and RNA from natural environments for analysis of ribosomal DNA- and rRNA-based microbial community composition. AEM 66(12): 5488–5499

Hamilton WA (2003) Microbially influenced corrosion as a model system for the study of metal microbe interactions: a unifying electron transfer hypothesis. Biofouling 19(1): 65–76

Hammes F, Boon N, de Villiers J, Verstraete W & Siciliano SD (2003) Strain-specific ureolytic microbial carbonate precipitation. Appl. Environ. Microbiol. 69(8): 4901–4909

Kawaguchi T & Decho AW (2002) A laboratory investigation of cyanobacterial extracellular polymeric secretions (EPS) in influencing $CaCO_3$ polymorphism. J. Cryst. Growth 240: 230–235

Kowalchuk GA, Bodelier PLE, Heilig GHJ, Stephen JR & Laanbroek HJ (1998) Community analysis of ammonia-oxidising bacteria, in relation to oxygen availability in soils and root oxygenated sediments, using PCR, DGGE and oligonucleotide probe hybridistation. FEMS Microbiol. Ecol. 27: 339–350

Merz-Preiss M & Riding R (1999) Cyanobacterial tufa calcification in two freshwater streams: ambient environment, chemical thresholds and biological processes. Sediment. Geol. 126(1–4): 103–124

Mobley HLY & Hausinger RP (1989) Microbial ureases: significance, regulation and molecular characterization. Microb. Rev. 53: 85–108

Molin J & Molin S (1997) CASE: complex adaptive systems ecology. Adv. Microb. Ecol. 15: 27–29

Prikryl R, Lokajicek T, Svobodova J & Weishauptova Z (2003) Experimental weathering of marlstone from Predni Kopanina (Czech Republic) – historical building stone of Prague. Build. Environ. 38: 1163–1171

Rowan NJ, Caldow G, Gemmell CG & Hunter IS (2003) Production of diarrheal enterotoxins and other potential virulence factors by veterinary isolates of *Bacillus* species associated with nongastrointestinal infections. Appl. Environ. Microbiol. 69(4): 2372–2376

Stocks-Fischer S, Galinat JK & Bang SS (1999) Microbiological precipitation of CaCO3. Soil Biol. Biochem. 31: 1563–1571

Tsuneda S, Jung J, Hayashi H, Aikawa H, Hirata A & Sasaki H (2003) Influence of extracellular polymers on electrokinetic properties of heterotrophic bacterial cells examined by soft particle electrophoresis theory. Colloid Surface B 29: 181–188

Udert KM, Larsen TA & Gujer W (2003) Estimating the precipitation potential in urine-collecting systems. Water Res. 37: 2667–2677

Warren LA, Maurice PA & Ferris FG (2001) Microbially mediated calcium carbonate precipitation: implications for interpreting calcite precipitation and for solid-phase capture of inorganic contaminants. Geomicrobiol. J. 18: 93–115

Warscheid T & Braams J (2000) Biodeterioration of stone: a review. Int Biodeter. Biodegr. 46: 343–368

Wen ZT & Burne RA (2002) Functional genomics approach to identifying genes required for biofilm development by *Streptococcus mutans*. Appl. Environ. Microbiol. 68(3): 1196–1203

Yates KK & Robbins LL (1999) Radioisotope tracer studies of inorganic carbon and Ca in microbially derived CaCO3. Geochim. Cosmochim. Acta. 63(1): 129–136